

# Solid Solutions of a Jahn–Teller Compound in an Undistorted Host. 4. Neutron and X-ray Single-Crystal Structures of Two Cr/Zn Tutton Salt Solid Solutions and the Observation of Disorder by Low-Temperature Neutron Diffraction

F. Albert Cotton,<sup>\*,1a</sup> Lee M. Daniels,<sup>1a</sup> Larry R. Falvello,<sup>\*,1b</sup> Carlos A. Murillo,<sup>\*,1a,c</sup> and Arthur J. Schultz<sup>\*,1d</sup>

Department of Chemistry, University of Costa Rica, Ciudad Universitaria, Costa Rica, Department of Inorganic Chemistry and Aragon Materials Science Institute, University of Zaragoza-CSIC, 50009 Zaragoza, Spain, Department of Chemistry and Laboratory for Molecular Structure and Bonding, Texas A&M University, College Station, Texas 77843, and Intense Pulsed Neutron Source, Argonne National Laboratory, Argonne, Illinois 60439

Received May 25, 1994<sup>®</sup>

Solid solutions of the ammonium Cr/Zn Tutton salt with two different compositions,  $(\text{NH}_4)_2[\text{Cr}_{0.10}\text{Zn}_{0.90}(\text{H}_2\text{O})_6](\text{SO}_4)_2$ , **1**, and  $(\text{NH}_4)_2[\text{Cr}_{0.22}\text{Zn}_{0.78}(\text{H}_2\text{O})_6](\text{SO}_4)_2$ , **2**, have been studied by single-crystal X-ray diffraction at room temperature and by single crystal time-of-flight neutron diffraction at 11–16 K for **1** and at 11–17 K for **2**. Composition was also characterized by atomic absorption, AA, analysis. The solid solutions crystallize in the monoclinic space group  $P2_1/c$ ,  $Z = 2$ , with the following cell dimensions, where in each case the room temperature X-ray value is given first followed by the low-temperature neutron value. For **1**:  $a = 6.249(2), 6.286(1) \text{ \AA}$ ;  $b = 12.508(3), 12.367(2) \text{ \AA}$ ;  $c = 9.237(2), 9.147(2) \text{ \AA}$ ;  $\beta = 106.82(2), 106.87(1)^\circ$ ;  $V = 691.1(3), 680.4(2) \text{ \AA}^3$ . For **2**:  $a = 6.252(1), 6.260(1) \text{ \AA}$ ;  $b = 12.503(1), 12.242(2) \text{ \AA}$ ;  $c = 9.247(1), 9.093(1) \text{ \AA}$ ;  $\beta = 106.77(1), 106.89(2)^\circ$ ;  $V = 692.1(1), 666.8(2) \text{ \AA}^3$ . The structure of **1** was refined to residuals of  $R = 0.0226$  and  $0.0670$  and quality of fit = 1.099 and 1.165 for X-ray and neutron data, respectively; the corresponding residuals for the X-ray and neutron structures of **2** are  $R = 0.0215$  and  $0.0682$ , and quality-of-fit = 1.057 and 0.994. The anisotropic displacement parameters of the oxygen and hydrogen atoms from the neutron diffraction studies are examined for their implications as to the presence or absence of disorder in the ligands about the composite Cr/Zn metal center. The results for composition **2**,  $x(\text{Cr}) = 0.22$ , clearly indicate the presence of disorder for the aqua ligand affected by Jahn–Teller distortion in the pure chromium complex. For composition **1**,  $x(\text{Cr}) = 0.10$ , the observation of disorder is not clear. The structures of **1** and **2** are isotopic at a given temperature, but the room-temperature and low-temperature structures differ subtly in the hydrogen bonding pattern.

## Introduction

Several years ago we reported having observed the formation of molecular solid solutions in crystalline mixtures comprising at once the two compounds *trans*- $\text{Cr}(\text{H}_2\text{O})_4(\text{Sac})_2$  and *trans*- $\text{Zn}(\text{H}_2\text{O})_4(\text{Sac})_2$  (Sac = saccharinate,  $\text{C}_7\text{H}_4\text{NO}_3\text{S}$ ).<sup>2</sup> The fundamental difference between these molecular solid solutions and the previously known solid solutions in extended nonmolecular structures, is that, in the former, the intermolecular forces that serve as the mediators of homogeneity are significantly weaker than the *intramolecular* bonds that are subject to distortion in adjusting to that homogeneity. In the case of the Cr/Zn saccharinates, we observed an apparent progressive suppression of the Jahn–Teller distortion at the chromium center as a function of composition.

Since that first report of the observation of solid solutions in molecular crystals, we have expanded our study of this phenomenon in two directions. In a first line of inquiry, we have pursued the study of other systems that form molecular solid solutions, with the aim of further characterizing the phenomenon itself. To date we have examined three systems consisting of varying compositions of Jahn–Teller active complexes dissolved in non-Jahn–Teller hosts. Besides the Cr/

Zn saccharinates, the other systems studied have been *trans*- $\text{Cr}/\text{Zn}(\text{H}_2\text{O})_4(\text{Nic})_2$  (Nic = nicotinate,  $\text{C}_6\text{H}_4\text{NO}_2$ )<sup>3</sup> and the ammonium Cr/Zn Tutton salt,  $(\text{NH}_4)_2[\text{Cr}/\text{Zn}(\text{H}_2\text{O})_6](\text{SO}_4)_2$ .<sup>4</sup>

In a second line of inquiry, we have attempted to establish rigorous procedures for the study of these systems by single-crystal X-ray diffraction, which until recently was the major analytical technique employed for these investigations. Most aspects of the use of single-crystal diffraction were addressed—from the preparation of homogeneous single crystals, through the collection of sufficiently precise X-ray data, the refinement of the mixed Cr/Zn sites, and the means of establishing the homogeneity of the overall structure—in order to achieve both accurate measures of composition and accurate characterizations of the changes in molecular geometry that accompany the formation of a solid solution. Above all, it was essential to address the question of homogeneity of the single-crystal samples. That is to say, leaving aside the expected differences in vibrational motion, to what degree are the geometrical parameters of Cr- and Zn-centered complexes either identical, or similar, or influenced by the presence of the other in the same crystal?

The existence of different geometries for chemically different entities occupying crystallographically equivalent sites would result in the appearance of disorder. The methods we have used

<sup>®</sup> Abstract published in *Advance ACS Abstracts*, October 15, 1994.

(1) (a) Texas A&M University. (b) University of Zaragoza. (c) University of Costa Rica. (d) Argonne National Laboratory.  
(2) Cotton, F. A.; Falvello, L. R.; Murillo, C. A.; Valle, G. Z. *Anorg. Allg. Chem.* **1986**, *540*–541, 67.

(3) Cotton, F. A.; Falvello, L. R.; Ohlhausen, E. L.; Murillo, C. A.; Quesada, J. F. Z. *Anorg. Allg. Chem.* **1991**, *598*–599, 53.

(4) Araya, M. A.; Cotton, F. A.; Daniels, L. M.; Falvello, L. R.; Murillo, C. A. *Inorg. Chem.* **1993**, *32*, 4853.

to establish the presence or absence of crystallographic disorder, based on X-ray diffraction data, have included contouring "omit maps," analyzing anisotropic displacement parameters, and locating and refining hydrogen atoms for any ligands for which disorder could possibly be present.

We report here the results of single-crystal neutron and X-ray diffraction analyses of two solid solutions of the Jahn–Teller active ammonium chromium Tutton salt in a zinc Tutton salt host. This study has provided an opportunity to characterize more thoroughly the phenomenon of solid solutions in molecular systems, in addition to establishing the extent of the validity of single-crystal X-ray diffraction in the study of such systems.

## Experimental Section

In the preparation of divalent chromium compounds, all operations were carried out under a nitrogen atmosphere using standard Schlenk techniques. Water was deionized, deoxygenated by prolonged refluxing in a nitrogen atmosphere, and distilled just before it was used. Metals were purchased from Johnson Matthey Electronics with a purity of 99.99% or better. Ammonium sulfate (Fisher Scientific) and sulfuric acid (Baker) were used as received. The stock aqueous chromium(II) solution<sup>5</sup>, SACR and CrSO<sub>4</sub>·5H<sub>2</sub>O,<sup>6</sup> were prepared as reported earlier. ZnSO<sub>4</sub>·H<sub>2</sub>O was crystallized by concentrating solutions made by dissolving zinc metal in sulfuric acid. Atomic absorption analyses were carried out on a Shimadzu A670 spectrophotometer.

**Preparation of Crystalline (NH<sub>4</sub>)<sub>2</sub>[Cr<sub>0.10</sub>Zn<sub>0.90</sub>(H<sub>2</sub>O)<sub>6</sub>](SO<sub>4</sub>)<sub>2</sub>, 1.** To ZnSO<sub>4</sub>·H<sub>2</sub>O (0.38 g, 2.1 mmol) and (NH<sub>4</sub>)<sub>2</sub>SO<sub>4</sub> (0.37 g, 2.9 mmol) were added 0.5 mL of concentrated H<sub>2</sub>SO<sub>4</sub>. The mixture was deoxygenated and then 8.5 mL of SACR was added. The solution was carefully layered with 1 mL of ethanol, and then it was cooled to 4 °C. After 3 days two large crystals were separated by filtration. All physical measurements, neutron diffraction, X-ray diffraction analysis, and atomic absorption spectroscopy were done on fragments taken from only one of those crystals. The combined weight of the crystals was 0.097 g.

**Preparation of Crystalline (NH<sub>4</sub>)<sub>2</sub>[Cr<sub>0.22</sub>Zn<sub>0.78</sub>(H<sub>2</sub>O)<sub>6</sub>](SO<sub>4</sub>)<sub>2</sub>, 2.** To ZnSO<sub>4</sub>·H<sub>2</sub>O (0.225 g, 1.25 mmol) and (NH<sub>4</sub>)<sub>2</sub>SO<sub>4</sub> (0.25 g, 1.89 mmol) was added concentrated sulfuric acid (0.5 mL). The mixture was deoxygenated and then 10 mL of water was added. The resulting solution was added to crystalline CrSO<sub>4</sub>·5H<sub>2</sub>O (0.625 g, 2.62 mmol). After stirring, a layer of ethanol (3.0 mL) was carefully added to the light blue solution. A week later a large light-blue single crystal was isolated. The block-shaped crystal was carefully cut. The larger, almost cubic portion [weighing 0.00410 g, (1.3 mm)<sup>3</sup>] was used in the neutron diffraction experiment. The smaller portions were used for the other experiments.

**X-ray Structure Determinations. Composition 1, x(Cr) = 0.10.** The crystal used for X-ray analysis was cleaved from a larger crystal, a fragment of which had been used as the sample for neutron diffraction analysis (*vide infra*). Diffraction data were collected in the manner described for the other solid solutions in this series.<sup>4</sup> For this sample a total of 4244 nonsystematically absent reflections were collected in the +*h*, ±*k*, ±*l* hemisphere. Due to the high scattering power of the crystal and the lack of a mechanical attenuator on the diffraction instrument, 25 strong, low-angle reflections flooded the detector and were therefore not included in the data set. Lorentz and polarization corrections were applied, as was an absorption correction based on  $\psi$ -scans of five reflections with Eulerian angle  $\chi$  near 90°. The averaging of 3784 observed reflections gave  $R_{int} = 0.0299$  and resulted in 2026 unique reflections.

The X-ray structure was developed in a routine manner.<sup>7</sup> All hydrogen atoms were located in a difference Fourier map and refined

**Table 1.** Crystal Data for (NH<sub>4</sub>)<sub>2</sub>[Cr<sub>0.10</sub>Zn<sub>0.90</sub>(H<sub>2</sub>O)<sub>6</sub>](SO<sub>4</sub>)<sub>2</sub>

	X-ray	neutron
formula	Cr <sub>0.10</sub> Zn <sub>0.90</sub> S <sub>2</sub> O <sub>14</sub> N <sub>2</sub> H <sub>20</sub>	
fw	400.32	
space group	P2 <sub>1</sub> /c	
<i>a</i> , Å	6.249(2)	6.286(1)
<i>b</i> , Å	12.508(3)	12.367(2)
<i>c</i> , Å	9.237(2)	9.147(2)
$\beta$ , deg	106.82(2)	106.87(1)
<i>V</i> , Å <sup>3</sup>	691.1(3)	680.4(2)
<i>Z</i>	2	
<i>d</i> <sub>calcd.</sub> , g/cm <sup>3</sup>	1.923	1.954
<i>T</i> , K	295	11–16
$\mu$ (Mo K $\alpha$ ), cm <sup>-1</sup>	20.76	
$\lambda$ , Å	0.710 73	
$\lambda$ range, Å		0.7–4.2
data collcn technique	$\omega$ -2 $\theta$	time-of-flight Laue <sup>a</sup>
$\mu$ (incoherent + coherent), cm <sup>-1</sup>		1.471
$\mu$ (abs, 1.8 Å), cm <sup>-1</sup>		2.050
transm factors: max, min	0.9993, 0.8649	
extinction param <i>g</i> , rad <sup>-1</sup> × 10 <sup>-4</sup>		0.024(4)
<i>R</i> <sup>b</sup>	0.0226(1916 $F_o^2 > 2\sigma(F_o^2)$ )	0.0670
wR2 <sup>c</sup>	0.0609	
<i>R</i> <sub>w</sub> <sup>d</sup>		0.0644
weighting function	$w^e$	$w^f$

<sup>a</sup> Using 30 × 30 cm<sup>2</sup> position-sensitive detector. <sup>b</sup>  $R = \sum ||F_o| - |F_c|| / \sum |F_o|$ . <sup>c</sup>  $wR2 = [\sum w(F_o^2 - F_c^2)^2 / \sum w(F_o^2)^2]^{1/2}$ . <sup>d</sup>  $R_w = [\sum w(F_o - F_c)^2 / \sum wF_o^2]^{1/2}$ . <sup>e</sup>  $w = \sigma^2(F_o^2) + 0.0283(\max(F_o^2, 0) + 2F_c^2)/3 + 0.18(\max(F_o^2, 0) + 2F_c^2)^3$ . <sup>f</sup>  $w = 4F_o^2(\sigma^2(F_o^2) + (0.04F_o^2)^2 + 5000)$ .

independently, each with its own isotropic displacement parameter. The program SHELXL-93<sup>8</sup> was used for the X-ray refinement. All data were used, and the refinement was based on  $F^2$  rather than on  $|F|$ . The residuals are reported in Table 1, which gives a summary of important crystallographic parameters. Since the *R* factor based on  $F^2$  falls in a range different from that of the more familiar crystallographic *R* factor, we also report the latter (for data with  $I > 2\sigma(I)$ ) in the table.

**Composition 2, x(Cr) = 0.22.** The crystal was obtained and handled in a manner similar to that for composition 1. In this case a total of 4261 non-systematically absent reflections were collected in the -*h*, ±*k*, ±*l* hemisphere. Averaging of 3629 reflections resulted in 2013 unique reflections with  $R_{int} = 0.016$ . The structure refinement procedure was exactly the same as for 1. Important data collection and structure refinement data are given in Table 2.

**Neutron Structure Determinations.** Single-crystal neutron diffraction data were gathered at the Intense Pulsed Neutron Source at Argonne National Laboratory on the single crystal diffractometer (SCD) beam line. The SCD instrument is a fixed-detector energy-dispersive instrument with a time- and position-sensitive detector. Neutrons are produced by the pulsed (30 Hz) spallation source at IPNS, and the SCD instrument uses the entire thermal spectrum of neutrons from each pulse. The instrument measures time-of-flight, which is related to the neutron wavelength by the de Broglie equation  $\lambda = (h/m)(t/l)$ , in which  $h$  is Planck's constant,  $m$  is the neutron mass, and  $t$  is the time of flight for path length  $l$ . The SCD position-sensitive neutron detector contains a <sup>6</sup>Li glass scintillator with dimensions of 30 × 30 cm<sup>2</sup>. For a given crystal setting, data are stored in a three-dimensional histogram in which each point has coordinates *x*, *y*, and *t*, which are the horizontal and vertical detector positions and the time-of-flight, respectively. There are 120 time-of-flight channels in each histogram, constructed in such a way that  $\Delta t/t$  has a constant value of 0.015. Each histogram comprises measurements of a three-dimensional block of reciprocal space, from neutrons in the wavelength range 0.7–4.2 Å. A detailed description of the SCD instrument and data collection and analysis procedures has

(5) Cotton, F. A.; Lewis, G. E.; Murillo, C. A.; Schowtzer, W.; Valle, G. *Inorg Chem.* **1984**, *23*, 4038.

(6) Cotton, F. A.; Daniels, L. M.; Murillo, C. A.; Zúñiga, L. A. *Eur. J. Solid State Inorg. Chem.*, accepted.

(7) Preliminary calculations were carried out on Local Area VAX clusters, with the commercial packages SDP/VAX V3.0 (under VMS V5.4) and (under VMS V5.5) SHELXTL-PLUS release 4.21V. Siemens Analytical X-ray Instruments, Inc., Madison, WI, 1990.

(8) (a) Sheldrick, G. M. SHELXL-93: FORTRAN-77 program for the refinement of crystal structures from diffraction data. University of Göttingen, 1993. (b) Sheldrick, G. M. *J. Appl. Crystallogr.* Manuscript in preparation.

**Table 2.** Crystal Data for  $(\text{NH}_4)_2[\text{Cr}_{0.22}\text{Zn}_{0.78}(\text{H}_2\text{O})_6](\text{SO}_4)_2$ 

	X-ray	neutron
formula	$\text{Cr}_{0.22}\text{Zn}_{0.78}\text{S}_2\text{O}_{14}\text{N}_2\text{H}_{20}$	
fw	398.79	
space group	$P2_1/c$	
<i>a</i> , Å	6.252(1)	6.260(1)
<i>b</i> , Å	12.503(1)	12.242(2)
<i>c</i> , Å	9.247(1)	9.093(1)
$\beta$ , deg	106.77(1)	106.89(2)
<i>V</i> , Å <sup>3</sup>	692.1(1)	666.8(2)
<i>Z</i>	2	
<i>d</i> <sub>calcd</sub> , g/cm <sup>3</sup>	1.914	1.986
<i>T</i> , K	293(2)	11–17
$\mu(\text{Mo K}\alpha)$ , cm <sup>-1</sup>	19.43	
$\lambda$ , Å	0.710 73	
$\lambda$ range, Å		0.7–4.2
data collcn technique	$\omega-2\theta$	time-of-flight Laue <sup>d</sup>
$\mu(\text{incoherent} + \text{coherent})$ , cm <sup>-1</sup>		1.501
$\mu(\text{abs, 1.8 Å})$ , cm <sup>-1</sup>		2.092
transm factors: max, min	0.999, 0.825	
Extinction parameter <i>g</i> , rad <sup>-1</sup> × 10 <sup>-4</sup>		0.036(4)
<i>R</i> <sup>a</sup>	0.0215(1796 <i>F</i> <sub>o</sub> <sup>2</sup> > 2 $\sigma$ ( <i>F</i> <sub>o</sub> <sup>2</sup> ))	0.0682
wR2 <sup>b</sup>	0.0632	
<i>R</i> <sub>w</sub> <sup>c</sup>		0.0499
weighting function	<i>w</i> <sup>e</sup>	<i>w</i> <sup>f</sup>

<sup>a</sup> using 30 × 30 cm<sup>2</sup> position-sensitive detector. <sup>b</sup>  $R = \sum |F_o| - |F_c| / \sum |F_o|$ . <sup>c</sup>  $wR2 = [\sum w(F_o^2 - F_c^2)^2 / \sum w(F_o^2)]^{1/2}$ . <sup>d</sup>  $R_w = [\sum w(F_o - F_c)^2 / \sum w(F_o^2)^{1/2}]^{1/2}$ . <sup>e</sup>  $w = [\sigma^2(F_o^2) + 0.0371(\max(F_o^2, 0) + 2F_o^2)/3 + 0.14(\max(F_o^2, 0) + 2F_o^2)^3]^{-1}$ . <sup>f</sup>  $w = \{4F_o^2/(\sigma^2(F_o^2) + (0.03F_o^2)^2 + 70)\} \min(F_o^2/F_c^2, F_c^2/F_o^2)$ .

been reported in the literature.<sup>9,10</sup> Sample temperature is controlled by a Displex closed-cycle helium refrigerator (Air Products and Chemicals, Inc., Model CS-202).

For the crystal of  $(\text{NH}_4)_2[\text{Cr}_{0.10}\text{Zn}_{0.90}(\text{H}_2\text{O})_6](\text{SO}_4)_2$ , **1**, an initial orientation matrix was obtained by an autoindexing algorithm<sup>11</sup> from peaks in one histogram. For intensity data collection, 25 histograms were measured—each for a different  $\chi$  and  $\phi$  crystal setting—in order to cover a unique quadrant of reciprocal space. Bragg peaks were integrated in three dimensions about their predicted locations and were corrected for the incident neutron spectrum, detector efficiency, and deadtime loss. Lorentz and absorption corrections were also applied.

For the crystal of  $(\text{NH}_4)_2[\text{Cr}_{0.22}\text{Zn}_{0.78}(\text{H}_2\text{O})_6](\text{SO}_4)_2$ , **2**, the treatment was identical to that for composition **1**, except that 28 histograms were measured at different values of  $\chi$  and  $\phi$ .

Both refinements were conducted via similar routes. In each case, the initial structural model consisted of atomic coordinates for non-hydrogen atoms, taken from an X-ray structure determination of an ammonium Tutton salt. This model was refined isotropically, and then all of the hydrogen atoms were located in a difference Fourier map. Neither structure presented any unusual problems. Scattering lengths for all atoms were taken from a literature compilation.<sup>12</sup> In the final least-squares analysis for each structure, a secondary extinction correction<sup>13</sup> (Type I, Lorentzian distribution) was included, and all atoms were refined with anisotropic displacement parameters. The treatment of the composite Cr/Zn site required special attention, and this is described in detail in the Discussion. The refinements converged with the residuals given in Table 1 for **1** and in Table 2 for **2**; the tables also contain other information pertinent to data collection and structure solution for the two samples. For **1**, positional and equivalent isotropic displacement parameters are given in Table 3; selected bond distances

(9) Schultz, A. J.; Van Derveer, D. G.; Parker, D. W.; Baldwin, J. E. *Acta Crystallogr., Sect. C* **1990**, C46, 276.

(10) Schultz, A. J. *Trans. Am. Cryst. Assoc.* **1987**, 23, 61.

(11) Jacobson, R. A. *J. Appl. Crystallogr.* **1986**, 19, 283.

(12) Sears, V. F. In *Methods of Experimental Physics, Neutron Scattering, Part A*, Skold, K.; Price, D. L., Ed.; Academic Press: Orlando, FL, 1986, Vol. 23, pp 521–550.

(13) Becker, P. J.; Coppens, P. *Acta Crystallogr., Sect. A* **1975**, A31, 417–425.

**Table 3.** Atomic Positional and Equivalent Isotropic Displacement Parameters from the X-ray (Roman Type) and Neutron (Italic Type) Structures of  $(\text{NH}_4)_2[\text{Cr}_{0.10}\text{Zn}_{0.90}(\text{H}_2\text{O})_6](\text{SO}_4)_2$ , **1**

atom	<i>x</i>	<i>y</i>	<i>z</i>	<i>U</i> <sub>eq</sub> <sup>a</sup> , Å <sup>2</sup>
Cr/Zn	0.0000 <i>0.0000</i>	0.0000 <i>0.0000</i>	0.0000 <i>0.0000</i>	0.0020(1) <i>0.0024(6)</i>
S	-0.2599(1) <i>-0.2642(6)</i>	0.3629(1) <i>0.3687(3)</i>	-0.0925(1) <i>-0.0871(5)</i>	0.0021(1) <i>0.0039(8)</i>
O(1)	0.1664(2) <i>0.1654(3)</i>	0.1089(1) <i>0.1083(2)</i>	0.1712(1) <i>0.1776(3)</i>	0.0030(1) <i>0.0071(5)</i>
O(2)	0.0337(2) <i>0.0332(3)</i>	0.1114(1) <i>0.1146(2)</i>	-0.1635(1) <i>-0.1619(3)</i>	0.0028(1) <i>0.0058(5)</i>
O(3)	0.3001(2) <i>0.2998(3)</i>	-0.0681(1) <i>-0.0680(2)</i>	-0.0001(1) <i>-0.0008(3)</i>	0.0026(1) <i>0.0061(5)</i>
O(4)	-0.4089(2) <i>-0.4124(3)</i>	0.2719(1) <i>0.2769(2)</i>	-0.0879(1) <i>-0.0773(3)</i>	0.0035(1) <i>0.0062(5)</i>
O(5)	-0.2160(2) <i>-0.2169(3)</i>	0.4236(1) <i>0.4333(2)</i>	0.0481(1) <i>0.0530(2)</i>	0.0043(1) <i>0.0069(5)</i>
O(6)	-0.3762(2) <i>-0.3825(3)</i>	0.4329(1) <i>0.4366(2)</i>	-0.2201(1) <i>-0.2199(2)</i>	0.0028(1) <i>0.0054(4)</i>
O(7)	-0.0492(2) <i>-0.0571(3)</i>	0.3229(1) <i>0.3254(2)</i>	-0.1150(1) <i>-0.1102(3)</i>	0.0031(1) <i>0.0064(5)</i>
N	0.3575(2) <i>0.3535(2)</i>	0.3479(1) <i>0.3410(1)</i>	0.1339(2) <i>0.1368(2)</i>	0.0031(1) <i>0.0070(3)</i>
H11	0.2856(46) <i>0.3184(7)</i>	0.0942(20) <i>0.0878(5)</i>	0.2060(26) <i>0.2255(6)</i>	0.0045(6) <i>0.022(1)</i>
H12	0.1031(40) <i>0.0962(9)</i>	0.1197(19) <i>0.1192(5)</i>	0.2295(27) <i>0.2578(6)</i>	0.0044(6) <i>0.022(1)</i>
H21	0.0215(38) <i>-0.0023(8)</i>	0.1697(21) <i>0.1882(4)</i>	-0.1437(26) <i>-0.1417(6)</i>	0.0041(6) <i>0.018(1)</i>
H22	-0.0382(38) <i>-0.0600(8)</i>	0.0999(17) <i>0.0981(5)</i>	-0.2457(27) <i>-0.2676(6)</i>	0.0037(5) <i>0.020(1)</i>
H31	0.3184(34) <i>0.3253(8)</i>	-0.1308(17) <i>-0.1445(4)</i>	0.0249(23) <i>0.0233(6)</i>	0.0031(5) <i>0.019(1)</i>
H32	0.3407(40) <i>0.3384(8)</i>	-0.0647(20) <i>-0.0573(5)</i>	-0.0745(29) <i>-0.0955(6)</i>	0.0051(6) <i>0.023(1)</i>
H1	0.4512(50) <i>0.4541(9)</i>	0.3449(23) <i>0.3219(5)</i>	0.0895(32) <i>0.0713(7)</i>	0.0064(8) <i>0.024(1)</i>
H2	0.2302(51) <i>0.1942(7)</i>	0.3365(24) <i>0.3302(6)</i>	0.0765(31) <i>0.0703(8)</i>	0.0059(7) <i>0.026(1)</i>
H3	0.3848(39) <i>0.3915(11)</i>	0.3050(21) <i>0.2925(5)</i>	0.2097(29) <i>0.2327(7)</i>	0.0050(6) <i>0.026(2)</i>
H4	0.3632(43) <i>0.3754(10)</i>	0.4146(24) <i>0.4214(4)</i>	0.1615(30) <i>0.1695(7)</i>	0.0059(7) <i>0.025(1)</i>

<sup>a</sup> The equivalent isotropic displacement parameter *U*<sub>eq</sub> is calculated as  $U_{eq} = \sum U_{ij} a_i a_j$ , *i, j* = 1, 3.

**Table 4.** Selected Bond Distances (Å) and Bond Angles (deg) from the X-ray (Roman Type) and Neutron (Italic Type) Structures of  $(\text{NH}_4)_2[\text{Cr}_{0.10}\text{Zn}_{0.90}(\text{H}_2\text{O})_6](\text{SO}_4)_2$ , **1**<sup>a</sup>

Cr/Zn—O(1)	2.118(1) <i>2.129(2)</i>	S—O(5)	1.460(1) <i>1.465(5)</i>
Cr/Zn—O(2)	2.110(1) <i>2.103(2)</i>	S—O(6)	1.479(1) <i>1.487(5)</i>
Cr/Zn—O(3)	2.059(1) <i>2.066(2)</i>	S—O(7)	1.478(1) <i>1.478(5)</i>
S—O(4)	1.479(1) <i>1.488(5)</i>		
O(2)—Cr/Zn—O(1)	88.88(5) <i>89.29(9)</i>	O(7)—S—O(4)	109.72(6) <i>108.9(3)</i>
O(3)—Cr/Zn—O(1)	90.89(5) <i>90.84(9)</i>	O(5)—S—O(6)	108.90(7) <i>109.5(3)</i>
O(3)—Cr/Zn—O(2)	89.62(5) <i>89.70(9)</i>	O(5)—S—O(7)	110.80(8) <i>111.0(3)</i>
O(5)—S—O(4)	109.44(8) <i>109.6(3)</i>	O(7)—S—O(6)	109.88(6) <i>109.9(3)</i>
O(4)—S—O(6)	108.04(7) <i>107.8(3)</i>		

<sup>a</sup> Numbers in parentheses are estimated standard deviations in the least significant digits.

and bond angles are given in Table 4, and the hydrogen bonding interactions are given in Table 5. For **2**, the positional parameters, selected distances and angles, and hydrogen bonds are given in Tables

**Table 5.** Hydrogen Bonding Interactions from the X-ray (Roman Type) and Neutron (Italic Type) Structures of  $(\text{NH}_4)_2[\text{Cr}_{0.10}\text{Zn}_{0.90}(\text{H}_2\text{O})_6](\text{SO}_4)_2 \cdot \mathbf{1}^a$ 

donor-H...acceptor	D...A, Å	D-H, Å	H...A, Å	D-H...A, deg	acceptor coords
O(1)-H(11)···O(6)	2.791(2)	0.74(3)	2.05(3)	172(2)	$1 + x, 1/2 - y, 1/2 + z$
	2.778(3)	0.968(5)	1.825(5)	167.6(6)	
O(1)-H(12)···O(7)	2.826(2)	0.77(3)	2.07(3)	170(2)	$x, 1/2 - y, 1/2 + z$
	2.824(3)	0.965(6)	1.879(6)	165.4(6)	
O(2)-H(21)···O(7)	2.757(2)	0.76(3)	2.00(3)	172(2)	$x, y, z$
	2.738(3)	0.968(5)	1.771(5)	176.9(5)	
O(2)-H(22)···O(5)	2.705(2)	0.78(2)	1.93(2)	178(2)	$x, 1/2 - y, -1/2 + z$
	2.692(3)	0.995(5)	1.696(5)	178.5(5)	
O(3)-H(31)···O(4)	2.703(2)	0.82(2)	1.89(2)	171(2)	$-x, -y, -z$
	2.718(3)	0.974(6)	1.751(5)	171.6(5)	
O(3)-H(32)···O(6)	2.760(1)	0.80(3)	1.97(3)	168(2)	$-x, -1/2 + y, -1/2 - z$
	2.750(3)	0.973(6)	1.790(6)	168.4(6)	
N-H(1)···O(4)	2.993(2)	0.81(3)	2.26(3)	151(3)	$1 + x, y, z$
	2.881(3)	1.017(6)	1.877(6)	168.6(5)	
N-H(1)···O(5)	3.139(2)		2.43(3)	147(3)	$1 + x, y, z$
	3.222(3)		2.531(6)	124.9(5)	
N-H(2)···O(7)	2.909(2)	0.83(3)	2.10(3)	164(3)	$x, y, z$
	2.902(2)	1.018(5)	1.926(6)	159.3(6)	
N-H(3)···O(4)	2.968(2)	0.86(3)	2.17(3)	155(2)	$1 + x, 1/2 - y, 1/2 + z$
	2.983(3)	1.032(6)	2.009(6)	156.5(6)	
N-H(4)···O(6)	2.849(2)	0.87(3)	1.98(3)	179(2)	$-x, 1 - y, -z$
	2.845(3)	1.036(6)	1.813(6)	174.0(5)	

<sup>a</sup> Numbers in parentheses are estimated standard deviations in the least significant digits.

**Table 6.** Atomic Positional and Equivalent Isotropic Displacement Parameters from the X-ray (Roman Type) and Neutron (Italic Type) Structures of  $(\text{NH}_4)_2[\text{Cr}_{0.22}\text{Zn}_{0.78}(\text{H}_2\text{O})_6](\text{SO}_4)_2 \cdot \mathbf{2}$ 

atom	x	y	z	$u_{\text{eq}}, \text{Å}^2$
Cr/Zn	0.0000	0.0000	0.0000	0.0020(1)
	0.0000	0.0000	0.0000	0.0031(7)
S	-0.2596(1)	0.3626(1)	-0.0924(1)	0.0022(1)
	-0.2649(7)	0.3678(3)	-0.0867(4)	0.0043(9)
O(1)	0.1676(2)	0.1097(1)	0.1718(1)	0.0032(1)
	0.1673(4)	0.1092(2)	0.1792(2)	0.0107(6)
O(2)	0.0331(2)	0.1115(1)	-0.1641(1)	0.0029(1)
	0.0319(4)	0.1144(2)	-0.1623(2)	0.0070(5)
O(3)	0.2989(2)	-0.0683(1)	-0.0008(1)	0.0027(1)
	0.2986(4)	-0.0684(2)	-0.0021(2)	0.0072(5)
O(4)	-0.4081(2)	0.2715(1)	-0.0882(1)	0.0036(1)
	-0.4118(4)	0.2766(2)	-0.0763(2)	0.0065(5)
O(5)	-0.2165(2)	0.4232(1)	0.0478(1)	0.0044(1)
	-0.2175(4)	0.4335(2)	0.0536(2)	0.0090(5)
O(6)	-0.3754(2)	0.4325(1)	-0.2198(1)	0.0029(1)
	-0.3811(4)	0.4363(2)	-0.2192(2)	0.0058(5)
O(7)	-0.0488(2)	0.3229(1)	-0.1146(1)	0.0033(1)
	-0.0568(4)	0.3252(2)	-0.1093(2)	0.0072(5)
N	0.3577(2)	0.3483(1)	0.1337(2)	0.0032(1)
	0.3531(2)	0.3410(1)	0.1373(1)	0.0081(3)
H11	0.2859(5)	0.0942(2)	0.2092(3)	0.0049(6)
	0.3211(8)	0.0887(4)	0.2277(4)	0.024(1)
H12	0.1092(4)	0.1238(2)	0.2338(3)	0.0037(5)
	0.0971(9)	0.1200(4)	0.2587(4)	0.023(1)
H21	0.0074(4)	0.1693(2)	-0.1446(3)	0.0040(5)
	-0.0036(9)	0.1890(3)	-0.1411(4)	0.021(1)
H22	-0.0438(4)	0.1025(2)	-0.2536(3)	0.0038(5)
	-0.0592(8)	0.0981(3)	-0.2672(4)	0.021(1)
H31	0.3265(4)	-0.1354(2)	0.0260(2)	0.0040(5)
	0.3244(8)	-0.1449(3)	0.0239(4)	0.019(1)
H32	0.3465(4)	-0.0652(2)	-0.0721(3)	0.0058(7)
	0.3363(8)	-0.0582(4)	-0.0965(4)	0.021(1)
H1	0.4535(5)	0.3418(2)	0.0869(3)	0.0065(8)
	0.4543(9)	0.3208(4)	0.0709(5)	0.025(1)
H2	0.2277(5)	0.3354(2)	0.0703(3)	0.0059(7)
	0.1932(8)	0.3311(4)	0.0696(5)	0.027(1)
H3	0.3858(4)	0.3068(2)	0.2067(3)	0.0056(7)
	0.3900(11)	0.2922(4)	0.2310(4)	0.029(2)
H4	0.3547(4)	0.4158(2)	0.1585(3)	0.0059(7)
	0.3741(9)	0.4213(3)	0.1698(5)	0.024(1)

<sup>a</sup> The equivalent isotropic displacement  $U_{\text{eq}}$  is calculated as  $U_{\text{eq}} = \sum U_{ij} a_i a_j a_k^2$ ,  $i, j = 1, 2, 3$ .

6–8, respectively. A thermal-ellipsoid plot of one asymmetric unit, taken from the neutron diffraction structure of **1**, is shown in Figure 1.

**Table 7.** Selected Bond Distances (Å) and Bond Angles (deg) from the X-ray (Roman Type) and Neutron (Italic Type) Structures of  $(\text{NH}_4)_2[\text{Cr}_{0.22}\text{Zn}_{0.78}(\text{H}_2\text{O})_6](\text{SO}_4)_2 \cdot \mathbf{2}^a$ 

Cr/Zn-O(1)	2.1312(1)	S-O(5)	1.4578(1)
	2.133(2)		1.463(4)
Cr/Zn-O(2)	2.1143(1)	S-O(6)	1.4774(1)
	2.085(2)		1.474(4)
Cr/Zn-O(3)	2.0568(1)	S-O(7)	1.4772(1)
	2.053(2)		1.477(5)
S-O(4)	1.4770(1)		
	1.463(5)		
O(2)-Cr/Zn-O(1)	88.97(4)	O(7)-S-O(4)	109.69(7)
	89.58(7)		109.5(3)
O(3)-Cr/Zn-O(1)	91.03(5)	O(5)-S-O(6)	108.94(7)
	90.97(8)		109.2(3)
O(3)-Cr/Zn-O(2)	89.65(4)	O(5)-S-O(7)	110.78(8)
	89.57(8)		110.5(3)
O(5)-S-O(4)	109.46(8)	O(7)-S-O(6)	109.87(6)
	109.6(2)		109.3(2)
O(4)-S-O(6)	108.05(7)		
	108.5(3)		

<sup>a</sup> Numbers in parentheses are estimated standard deviations in the least significant digits.

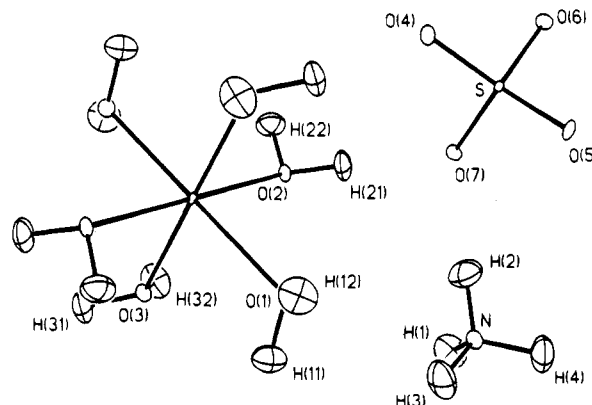


**Figure 1.** Thermal ellipsoid plot of one asymmetric unit of  $(\text{NH}_4)_2[\text{Cr}_{0.10}\text{Zn}_{0.90}(\text{H}_2\text{O})_6](\text{SO}_4)_2$ , showing the atom naming scheme, from the determination by neutron diffraction. Atoms are represented by their 50% probability ellipsoids.

## Results and Discussion

**Population Refinement.** In earlier reports<sup>2–4</sup> we discussed the questions of significance and determinacy in the refinement

**Table 8.** Hydrogen Bonding Interactions from the X-ray (Roman Type) and Neutron (Italic Type) Structures of  $(\text{NH}_4)_2[\text{Cr}_{0.22}\text{Zn}_{0.78}(\text{H}_2\text{O})_6](\text{SO}_4)_2$ , **2**<sup>a</sup>

donor-H...acceptor	D...A, Å	D-H, Å	H...A, Å	D-H...A, deg	acceptor coords
O(1)-H(11)···O(6)	2.791(2) 2.765(3)	0.75(3) 0.963(5)	2.06(3) 1.818(5)	169(2) 167.0(4)	1 + x, 1/2 - y, 1/2 + z
O(1)-H(12)···O(7)	2.826(2) 2.807(3)	0.78(2) 0.962(5)	2.05(2) 1.864(5)	174(2) 165.8(4)	x, 1/2 - y, 1/2 + z
O(2)-H(21)···O(7)	2.756(2) 2.710(3)	0.77(2) 0.970(5)	1.99(2) 1.741(4)	174(2) 176.4(4)	x, y, z
O(2)-H(22)···O(5)	2.706(2) 2.666(3)	0.84(2) 0.981(4)	1.87(2) 1.685(4)	178(2) 178.4(4)	x, 1/2 - y, -1/2 + z
O(3)-H(31)···O(4)	2.697(2) 2.688(3)	0.88(2) 0.963(4)	1.82(2) 1.732(4)	175(2) 171.4(5)	-x, -y, -z
O(3)-H(32)···O(6)	2.759(1) 2.730(2)	0.80(3) 0.965(4)	1.98(3) 1.777(4)	164(2) 168.7(5)	-x, -1/2 + y, -1/2 - z
N-H(1)···O(4)	3.002(2) 2.868(2)	0.84(3) 1.024(4)	2.23(3) 1.854(4)	154(2) 169.4(5)	1 + x, y, z
N-H(1)···O(5)	3.133(2) 3.206(3)		2.42(3) 2.515(6)	143(2) 124.3(4)	1 + x, y, z
N-H(2)···O(7)	2.909(2) 2.883(3)	0.87(3) 1.017(5)	2.06(3) 1.905(5)	167(2) 160.3(4)	x, y, z
N-H(3)···O(4)	2.971(2) 2.965(2)	0.83(3) 1.013(4)	2.19(3) 2.012(5)	157(2) 155.8(5)	1 + x, 1/2 - y, 1/2 + z
N-H(4)···O(6)	2.847(2) 2.819(2)	0.88(3) 1.017(4)	1.97(3) 1.805(5)	175(2) 174.2(5)	-x, 1 - y, -z

<sup>a</sup> Numbers in parentheses are estimated standard deviations in the least significant digits.

of the populations of mixed Cr/Zn sites of single-crystal X-ray diffraction data. We also considered the possibility of a small bias that could appear in the population parameter as a result of the use of a single set of thermal displacement parameters for the composite site, since the lighter Cr atoms will have larger displacements than the heavier Zn atoms.

In the X-ray structures of  $(\text{NH}_4)_2[\text{Cr}_x\text{Zn}_{1-x}(\text{H}_2\text{O})_6](\text{SO}_4)_2$  reported here, the refinement once again provides the usual indications of significance and determinacy. That is to say, if a composition different from  $\text{Cr}_{0.10}\text{Zn}_{0.90}$  is forced upon the structural model of **1**, for example, then a noteworthy worsening of the least-squares residuals is observed (significance), and refinements beginning with quite different values of the population parameter all converge to the same result (determinacy). What is more, the result agrees nicely with the AA analysis. We have stated that these properties of the X-ray refinement have their origins in the fact that the difference between the scattering factors of chromium and zinc ( $f_{\text{Cr}} - f_{\text{Zn}}$ ) is not a simple function of  $(\sin \theta)/\lambda$ . Thus, the refinement does not suffer from an inverse functional correlation between  $x(\text{Cr})$  and the displacement parameters of the Cr/Zn site.

In the refinements of the low-temperature neutron data, the compositions at the metal sites were fixed at the values found in the room-temperature X-ray diffraction analyses. When refined freely using the low temperature neutron diffraction data, the composition of the Cr/Zn site in **1** refined to  $x(\text{Cr}) = 0.19(1)$ . When  $x(\text{Cr})$  was varied within the range 0.05–0.20, we observed changes in the magnitudes of the displacement parameters for the metal-atom site without significant changes in the least-squares residuals. We believe the correlation between the composition parameter and the displacement factors in the case of the neutron data analysis is due to the small magnitudes of the temperature factors at 11–16 K. Thus, small changes in the composition parameter could result in small, but proportionally significant, changes in the temperature factors. At room temperature, small changes in the large temperature factors would not be significant. Since the refinement of population was not the principal aim of the neutron diffraction analysis, the value for  $x(\text{Cr})$  obtained by atomic absorption spectroscopy and room temperature X-ray diffraction of 0.10 was fixed in the final neutron refinement for sample **1**. For sample **2**, to which we attribute a composition of  $x(\text{Cr}) = 0.22(1)$  based on

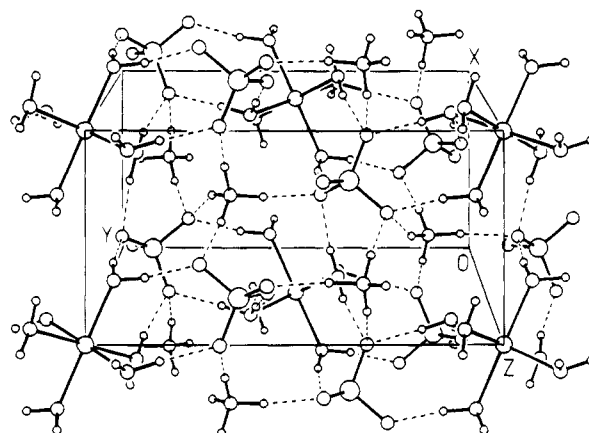


**Figure 2.** Packing plot of the crystal structure of  $(\text{NH}_4)_2[\text{Cr}_{0.10}\text{Zn}_{0.90}(\text{H}_2\text{O})_6](\text{SO}_4)_2$ , from the determination by neutron diffraction. The lattice plane (100) is in the plane of the paper.

the X-ray analysis, a free refinement of composition to the neutron data had given a result of  $x(\text{Cr}) = 0.20(4)$ .

**Structure Types.** There is a small difference between the isotopic room-temperature X-ray structures and the low-temperature structures that we have determined by neutron diffraction, which are also isotopic but which are different from the room-temperature structure. In Table 5, which lists the hydrogen bonds for the X-ray and neutron structures of **1**, the interaction at N-H(1), a bifurcated hydrogen bond in the X-ray structure, is seen to be dominated by one of its components at low temperature. This same difference holds in the structures determined for **2**, as can be seen in the listing of hydrogen bonds in Table 8. The change of structural type accompanies a change of temperature and is not associated with the difference in composition between **1** and **2**.

In all cases, the  $[\text{Cr}/\text{Zn}(\text{H}_2\text{O})_6]^{2+}$  complexes are held in a constraining environment by a rich network of hydrogen bonds. Figure 2 shows part of the extended structure, taken from the neutron structure of **1**, with the hydrogen bonds indicated. All of the hydrogen atoms in the structure, including the 12 atoms of the  $[\text{M}(\text{H}_2\text{O})_6]^{2+}$  group, are donors in hydrogen bonds. It will be this network of energetic interactions that mediates any change in the Jahn-Teller effect at the chromium centers,

including the switching of the M–O bond elongation from M–O(2) in the pure Cr system to M–O(1) in the solid solutions.

The selected distances and angles given in Tables 4 and 7 for **1** and **2**, respectively, show that there is essentially no difference in the covalent structure revealed by the four determinations reported here, except of course in the apparent bond distances at the metal center. The latter vary with composition, as a result of disorder.

We observe an almost uniform difference of  $1/5$  Å between the covalently bonded distances involving hydrogen determined by neutron diffraction and those determined by X-ray diffraction. This result, which is expected, is clearly seen in the tables of hydrogen bonds, Tables 5 and 8. The hydrogen atom positions determined by X-ray diffraction are in all cases along the same O–H or N–H vector seen by neutron diffraction, and displaced toward the parent atom. The uniformity of the displacements in these structures and in the structure of  $\text{VSO}_4 \cdot 7\text{H}_2\text{O}$  reported in the accompanying paper<sup>14</sup> emphasize the precision with which accurate X-ray data can define the part of the hydrogen atom visible to X-ray diffraction.<sup>15</sup>

**Displacement Parameters—Observation of Disorder.** The principal reason for undertaking the neutron structure determinations of  $(\text{NH}_4)_2[\text{Cr}_x\text{Zn}_{1-x}(\text{H}_2\text{O})_6](\text{SO}_4)_2$  was to attempt to observe any disorder that might arise in the ligands affected by Jahn–Teller distortion at the chromium center—in this case, the aqua ligands containing O(1) and/or O(2). On one hand, it would be expected that a clearer picture of all important structural features, including static disorder if it were present, would emerge at the low temperature of the neutron data collection. In addition, the precise location and displacement parameters of the hydrogen nuclei of these ligands allows a more thorough examination of the behavior of all of the atoms of the ligands under scrutiny and provides a broader base for comparison of these ligands with entities known to be ordered, such as the aqua ligand containing atom O(3).

We see in the anisotropic displacement parameters of sample **2** ( $x(\text{Cr}) = 0.22$ ) a clear indication of disorder in atom O(1) of the ligand affected by Jahn–Teller elongation in the pure chromium complex. (As noted in a previous report<sup>4</sup> upon formation of the solid solutions the Jahn–Teller effect is switched from elongation of the M–O(2) bond to elongation of M–O(1). For present purposes we thus treat O(1) as the atom affected by Jahn–Teller distortion; but where needed the figure used for the elongated bond distance in a pure Cr sample will be that reported for Cr–O(2) in the previous paper.) Figure 3 shows the elongation of the displacement ellipsoid for atom O(1) in the low-temperature neutron structure of **2**. The principal RMS displacements<sup>16</sup> of O(1) in this structure have values of 0.085(5), 0.095(5), and 0.124(4) Å. Unlike the situation for atoms O(2) and O(3), for which the largest principal displacements are roughly transverse to the M–O bond, in the case of O(1) the direction of the largest principal displacement is roughly parallel to M–O(1), making an angle of  $15(6)^\circ$  with the latter. For O(2) and O(3), the largest principal displacements have rms (root mean square) values of 0.101(5) and 0.100(4) Å, respectively, and make angles of  $85(8)^\circ$  and  $103(17)^\circ$  with their respective M–O bonds. Given the general character of the displacement ellipsoids of the rest of the atoms in the structure, we conclude that the elongation of O(1) is caused by

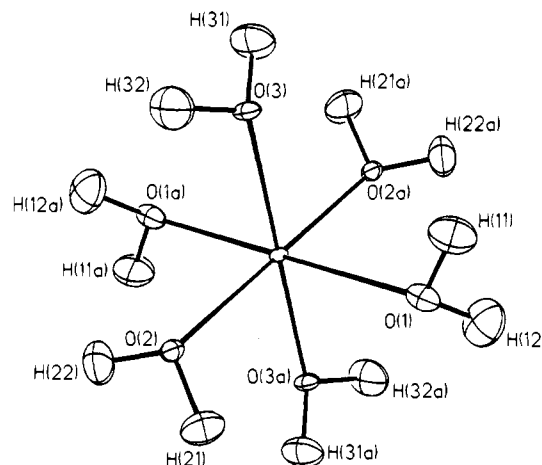


**Figure 3.** Thermal ellipsoid plot of the cation  $[\text{M}(\text{H}_2\text{O})_6]^{2+}$  from the neutron structure of  $(\text{NH}_4)_2[\text{Cr}_{0.22}\text{Zn}_{0.78}(\text{H}_2\text{O})_6](\text{SO}_4)_2$ , **2**. Atoms are represented by their 60% probability ellipsoids. The elongation of the ellipsoid for atom O(1) is clearly visible.

disorder. That is, the behavior of the congener of O(1) that is bonded to Cr is different from that of the congener bound to Zn.

Any attempt at further characterization of this disorder requires an assumption about its nature. We consider first the possibility of static disorder. In this case, the mean position we observe for O(1) would be a weighted mean of the separate positions of O(1)(Cr) and O(1)(Zn), each of which in its turn would reside at a position determined by its distinct potential energy minimum. To effect a rough quantitative analysis of this situation—that is, to estimate the separation between the two disordered congeners—we shall make use of the difference mean-square displacement amplitudes between pairs of atoms,  $\Delta\text{MSDA}$ , calculated from the structural results of the neutron study of sample **2**. A  $\Delta\text{MSDA}$  value is the difference in the mean-square displacements of two atoms along their interatomic vector. Stebler and Bürgi<sup>17</sup> have presented a rigorous analysis of the effects of disorder on displacement parameters. Among others, they give the following formula relating apparent atomic displacements and the separation of the mean positions of the disordered congeners. Without changing the formula, we present it here in notation appropriate to the present study (eq 1). In the Equation,  $\Delta U_{\text{dis}}$  is the difference in mean-square

$$\Delta U_{\text{dis}} \approx 4x(\text{Cr})(1 - x(\text{Cr}))\Delta d^2(\text{M}-\text{O}) \quad (1)$$

displacement amplitudes (along the interatomic vector) between the metal and ligand atom sites, caused by the distribution of the ligand atom over two disordered, but not resolved, positions. It is obtained by subtracting, from the  $\Delta\text{MSDA}$  value, the contribution to  $\Delta\text{MSDA}$  of any features other than the distribution of the ligand atom over two sites. The quantity  $\Delta d$  is half of the difference between the two bond distances at the same site, in this case Cr–O(1) and Zn–O(1). In the present case, the  $\Delta\text{MSDA}$  value for M–O(1) is  $127 \times 10^{-4} \text{ \AA}^2$  while those for M–O(2) and M–O(3) are  $11 \times 10^{-4}$  and  $15 \times 10^{-4} \text{ \AA}^2$ , respectively. (The  $\Delta\text{MSDA}$  values were calculated by program THMA11.)<sup>18</sup> Subtracting the larger of the two values for the nondisordered sites from the  $\Delta\text{MSDA}$  value for M–O(1), we estimate  $\Delta U_{\text{dis}}$  as  $112 \times 10^{-4} \text{ \AA}^2$  for the latter. Then for  $x(\text{Cr}) = 0.22$ , we obtain a value of 0.26 Å for  $2\Delta d$ , the difference between  $d(\text{Cr}-\text{O}(1))$  and  $d(\text{Zn}-\text{O}(1))$ . This compares well with

(14) Cotton, F. A.; Falvello, L. R.; Murillo, C. A.; Pascual, I.; Schultz, A. J.; Tomás, M. *Inorg. Chem.*, preceding paper in this issue.

(15) Cotton, F. A.; Luck, R. L. *Inorg. Chem.* **1989**, *28*, 3210.

(16) Busing, W. R.; Martin, K. O.; Levy, H. A. ORFFE: A crystallographic function and error program. Oak Ridge National Laboratory, 1971.

(17) Stebler, M.; Bürgi, H. B. *J. Am. Chem. Soc.* **1987**, *109*, 1395.

(18) (a) Dunitz, J. D.; Schomaker, V.; Trueblood, K. N. *J. Phys. Chem.* **1988**, *92*, 856. (b) Trueblood, K. N. Private communication, 1992.

**Table 9.** Principal Rms Displacements (Å) for Selected Atoms from the Neutron Crystal Structures of  $(\text{NH}_4)_2[\text{Cr}_{0.10}(\text{H}_2\text{O})_6](\text{SO}_4)_2$ , **1**, and  $(\text{NH}_4)_2[\text{Cr}_{0.22}\text{Zn}_{0.78}(\text{H}_2\text{O})_6](\text{SO}_4)_2$ , **2**

atom		principal axis			rms <sup>a</sup>
		1	2	3	
O(1)	1	0.060(7)	0.087(5)	0.101(4)	0.092(5)
	2	0.085(5)	0.095(5)	0.124(4)	0.122(4)
H(11)	1	0.121(6)	0.155(6)	0.167(7)	0.150(7)
	2	0.104(9)	0.163(5)	0.183(7)	0.165(6)
H(12)	1	0.104(9)	0.161(7)	0.175(9)	0.162(7)
	2	0.118(7)	0.159(6)	0.174(6)	0.161(6)
O(2)	1	0.057(7)	0.077(6)	0.090(4)	0.061(7)
	2	0.070(6)	0.078(4)	0.101(5)	0.077(4)
H(21)	1	0.079(9)	0.144(7)	0.161(6)	0.135(8)
	2	0.093(8)	0.150(5)	0.180(7)	0.140(6)
H(22)	1	0.109(6)	0.153(7)	0.156(8)	0.146(8)
	2	0.103(5)	0.146(7)	0.165(7)	0.137(5)
O(3)	1	0.063(7)	0.076(4)	0.093(5)	0.070(5)
	2	0.059(8)	0.088(4)	0.100(4)	0.063(7)
H(31)	1	0.094(9)	0.150(7)	0.163(6)	0.143(7)
	2	0.098(7)	0.142(7)	0.161(6)	0.138(7)
H(32)	1	0.106(10)	0.151(7)	0.189(7)	0.145(7)
	2	0.105(7)	0.139(8)	0.188(6)	0.135(8)

<sup>a</sup> The final column gives the rms displacement parallel to the nearest M—O bond.

the difference between the relevant Cr—O and Zn—O distances, 0.213(2) Å, taken from room-temperature X-ray data from the pure Cr and Zn Tutton salts.<sup>4</sup> Because the population at the metal center is not evenly divided between chromium and zinc, we cannot make a clean estimation of the actual M—O distances.

Although sample **1** contains only 10% chromium, we also see an elongation of the displacement of atom O(1) in the direction of the M—O bond, in comparison to what is seen for O(2) and O(3). The values of  $\Delta\text{MSDA}$  for M—O(1), M—O(2), and M—O(3) are  $70 \times 10^{-4}$ ,  $13 \times 10^{-4}$ , and  $14 \times 10^{-4}$  Å<sup>2</sup>, respectively. Using the same procedure as for sample **2**, we obtain a value of 0.25 Å for the difference between Cr—O(1) and Zn—O(1). This agrees well with the value calculated for sample **2**, although we would not have put much stock in the value calculated from the sample with small  $x(\text{Cr})$ , if it were the only one at hand.

A second possible explanation for the observed disorder is that the relatively static structure of the pure zinc compound is superposed on a dynamic Jahn—Teller effect in the chromium compound. It is already clear that something unusual happens to the chromium complex upon incorporation in the zinc host, because we observe distortion switching from Cr—O(2) to Cr—O(1). Switching of the expression of the Jahn—Teller effect from static to dynamic is another plausible response to a constraining environment. We do not attempt a rigorous analysis of the displacement parameters for this model. The idea of dynamic disorder gains credence from the separation of roughly  $1/4$  Å calculated from the model for static disorder. This is a separation that we would expect to be able to resolve at low temperature if the disorder were static. With dynamic disorder, the elongation of the displacement ellipsoid would represent a continuum of vibrational displacement that would not be resolved at any temperature.

In Table 9 are gathered the principal RMS displacements of the nine atoms of the three aqua ligands, taken from the two neutron analyses. The final column of the table gives the RMS displacement of each of these atoms in a direction parallel to the metal—oxygen bond to the ligand containing the atom. For sample **1**, there is a rather slight augmentation of the values for O(1), H(11), and H(12). It is a small enough effect that in the absence of other reasons to suspect disorder, we would not be inclined to read too much into the numbers. For O(1) in sample

**2**, however, the effect is clear. The RMS displacement parallel to M—O(1) is significantly larger in sample **2**, as would be expected for the larger  $x(\text{Cr})$  in the presence of disorder. Interestingly, the increase in the RMS displacement parallel to M—O(1) is barely significant for H(11), and the number actually decreases (though by an insignificant amount) for H(12). There are other factors at work in the displacement parameters of hydrogen atoms seen with neutron diffraction, making it imprudent to draw rigorous conclusions from numbers such as these. Nevertheless, these numbers, along with the constraining environment in which the hydrogen atoms lie, favor a conclusion of dynamic disorder at the metal center. A dynamic disorder could well have a larger effect on O(1) than on the two hydrogen atoms attached to it, as the latter are constrained by hydrogen bonds.

One of the questions that we wanted to address with this study was whether X-ray diffraction data, particularly at room temperature, are capable of exposing subtle disorder in these molecular solid solutions. The present results indicate that they are. Looking first at the room temperature X-ray results for sample **1**, we use the  $\Delta\text{MSDA}$  values of the S—O bonds of the sulfate group as a gauge of whether the displacement parameters have any comparative value at all. The  $\Delta\text{MSDA}$ 's for the four S—O bonds are  $1 \times 10^{-4}$ ,  $1 \times 10^{-4}$ ,  $4 \times 10^{-4}$ , and  $-3 \times 10^{-4}$  Å<sup>2</sup>—values which clearly indicate that the data are capable of exposing the rigidity of the group. The  $\Delta\text{MSDA}$ 's at the metal center (in units of  $10^{-4}$  Å<sup>2</sup>) are 53, 23, and 17 for M—O(1), M—O(2), and M—O(3), respectively. This does indeed expose an elongation of the displacement of O(1) parallel to the M—O bond. For sample **2**, for which the higher concentration of Cr should as before lead to a more pronounced effect, we calculate  $\Delta\text{MSDA}$ 's of  $82 \times 10^{-4}$ ,  $42 \times 10^{-4}$ , and  $22 \times 10^{-4}$  Å<sup>2</sup> for M—O(1), M—O(2), and M—O(3), respectively. For the sulfate group, the four values are  $5 \times 10^{-4}$ ,  $5 \times 10^{-4}$ ,  $0 \times 10^{-4}$ , and  $-2 \times 10^{-4}$  Å<sup>2</sup>. The numbers for M—O show qualitatively what would be expected for a case of either static or dynamic disorder, present to a greater extent than in sample **1**. We conclude that the X-ray data are capable of exposing the disorder where it exists, even in the low- $x(\text{Cr})$  sample. It is clear, however, that a quantitative examination of the results requires data at more than one temperature. The X-ray results show a less pronounced effect than that seen with low-temperature neutron data.

### Concluding Remarks

The data presented here establish two important conclusions—(1) that the structures of the mixed Cr/Zn Tutton salts are disordered at the aqua ligand affected by Jahn—Teller distortion in the chromium complex and (2) that room temperature X-ray diffraction data are capable of showing the presence of disorder. It remains to be established whether the disorder is static, dynamic, or a combination of both.

The results of this study leave open the possibility of more than one type of disorder. We observe two different kinds of behavior for the atoms of the  $e_g$  plane, O(1) and O(2). In both of the X-ray structures and in the neutron structure of sample **1**, the M—O(1) and M—O(2) distances are quite similar, and have values lying in the relatively narrow range 2.103(2)—2.131(1) Å. Taken alone, this might lead to a conclusion that the distances observed are "apparent" distances and that the Jahn—Teller effect is dynamic at the chromium centers in the solid solutions. However, the displacement parameters are elongated parallel to the M—O bond for O(1) alone. In the neutron structure of sample **2**, in contrast, we see clearly different behavior in terms of the static, apparent geometry, while the displacement parameters of O(1) even more clearly represent a

distribution elongated parallel to the M–O vector. The apparent M–O(1) distance lies near the range for the other M–O bonds, at 2.133(2) Å. The M–O(2) distance, however, is foreshortened to 2.085(2) Å. This is a significant change, and we take it as evidence that, in the higher Cr concentration sample at low temperature, the Jahn–Teller effect at the chromium center is again cooperative, or “frozen out” as it would be in a pure Cr sample and that the disorder in this case is static.

**Acknowledgment.** This work has benefited from the use of the Intense Pulsed Neutron Source at Argonne National Laboratory, which is funded by the U.S. Department of Energy, BES-

Materials Science, under Contract W-31-109-ENG-38. Financial support from the Department of Chemistry, University of Costa Rica, the Robert A. Welch Foundation (Grant No. A-494), and the Comisión Interministerial de Ciencia y Tecnología (Spain) (Project PB92-0360) is gratefully acknowledged. We also thank Ms. N. M. Alfaro and Ms. M. Bravo for their assistance in the atomic absorption measurements.

**Supplementary Material Available:** Tables of crystallographic data, complete bond distances and bond angles, anisotropic displacement parameters, and  $\Delta$ MSDA (14 pages). Ordering information is given on any current masthead page.